Aspects of electronic bonding under pressure: electron localization in symmetric double well model

Trinidad Novoa, Julia Contreras-García, Patricio Fuentealba, Carlos Cárdenas

Aspects of electronic bonding under pressure: electron localization in symmetric double well model

Trinidad Novoa[1], Julia Contreras-García[2]*, Patricio Fuentealba[1,3] and Carlos Cárdenas[1,3]*

1. *Departamento de Física, Facultad de Ciencias, Universidad de Chile, Casilla 653, Santiago, Chile.*
2. *Sorbonne Universités, UPMC, Laboratoire de Chimie Théorique and CNRS UMR CNRS 7616*
3. *Centro para el Desarrollo de la Nanociencia y la Nanotecnología (CEDENNA), Avda. Ecuador 3493, Santiago 9170124, Chile.*

Abstract

It has become recently clear that chemical bonding under pressure is still lacking guiding principles for understanding the way electrons reorganize when their volume is constrained. As an example, it has recently been shown that simple metals can become insulators (*aka* electrides) when submitted to high enough pressures. This has lead to the general believe that "a fundamental yet empirically useful understanding of how pressure alters the chemistry of the elements is lacking" (Hemley, 2010). We will show that a simple 1-dimensional double well potential with non-interacting electrons and its Electron Localization Function (ELF) mimic the sequence of chemical bonding undergone by atomic solids under pressure. First transforming into metals (predicted already in 1935) and finally to an electride form. This simple model provides a fast and visual framework for transformations in the electronic structure in the high-pressure regime in terms of two chemically sound parameters related to external potential and confinement. We are interested in understanding the role the Pauli principle plays on the localization/delocalization of non-interacting confined electrons.

I. INTRODUCTION

Confinement can dramatically change the microscopic structure of electronic systems because it increases the electrostatic repulsion between electrons and also makes Pauli repulsion more relevant.[1, 2] This leads to radically new materials with exotic and unexpected properties.[3] [4] As a recent example, superconductivity has shown to become common even in small and well known molecular solids such as H_2S.[5]

Moreover, some of these properties can be exploited at normal pressure by achieving metastable phases upon decompression cycles.[6] All these emerging properties underlie electronic structure changes which do not follow the normal pressure rules. E.g., at normal pressure electrons are known to organize in pairs, so that bonds and lone pairs are formed. These lone pairs usually lead to open structures (molecular solids, layers, channels) because the repulsion between pairs favors extended regions of low density. These open electronic structures are too voluminous and become unfavorable under pressure. Hence, new phases appear under pressure. Weak intermolecular interactions that glue molecular solids together transform under pressure into strong bonds leading to 3D extended solids.[4] As already predicted in 1935,[7] high pressures lead to increasing orbital overlap in these extended solids, so that the bandgap closes. In other words, solids should turn metallic at high enough pressures. With the advent of new pressure technologies it has been recently shown that the phase diagram of solids can be extended beyond metallization. An insulating pseudo-ionic state (aka electride) provides great stability for metals at very-high-pressure.[8, 9] In a solid-state electride, electrons occupy voids in the crystal structure, playing the role of the anion in an ionic crystal.[10] In other words, the pairing of electrons becomes once again, the most stable electronic arrangement.

Although these observations have been all simulated and verified in the laboratory, a general theory of chemical bond under pressure to follow these sequences of transformations is still in its very early days. As pointed out by Hemley, "a fundamental yet empirically useful understanding of how pressure alters the chemistry of the elements is lacking".[11]

II. THEORETICAL FRAMEWORK

A. The model: the symmetric double well potential

We would like to work on a simple model of non-interacting electrons that enables to follow the above series of transformations, providing greater insight into electronic organization under pressure or confinement.

In order to do so, one has to model the interplay of potential and kinetic contributions upon pressurization. However, a main issue arises when analyzing the

potential-kinetic energy balance along the periodic table. Properties behave in a non-continuous manner as atomic number changes. The simultaneous increase of number of electrons and protons along the periodic table and the quantum filling of shells make it difficult sometimes to understand and isolate which effects are due to the external potential (number and position of nuclei) and which ones to the Pauli principle. This rationale has also been recently adopted in the so-called "quantum chemical alchemy", where continuous changes in the atomic charge have been simulated.[12-16]

One way to avoid the complexities of discontinuous changes of atomic properties is through the development of simple quantum models that resemble atomicity (atoms in molecules and solids) but whose parameters are continuous variables. Here, we resort to a polynomial symmetric double well (SDW) potential with barrier height V_0 and distance between the bottoms of wells 2λ (see Scheme 1). For simplicity, we will use the following notation: SDW(V_0,λ) where V_0 is in hartree (E_h) and λ in bohr (a_o). This model has been previously used to understand proton tunneling, inversion of ammonia and even hydrogen bonding in DNA.[17] [18] Note, there are numerous double-well potentials such as the multiple-square (periodic) wells used by Kronig-Penney to model metals.[19]

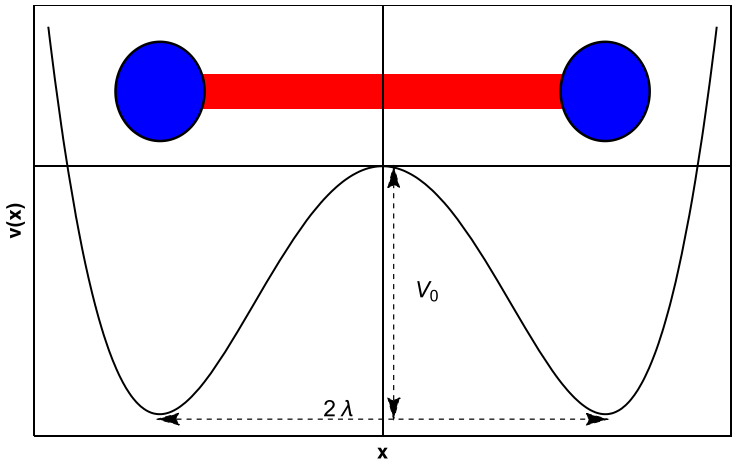

Scheme 1.

The shape of a polynomial symmetric double well potential is determined by two parameters: the depth of the well relative to the barrier, V_0, and the width of the barrier at the bottom of the wells, 2λ.

Despite its apparent simplicity there is no analytical solution to the Schrödinger equation of the SDW potential.[20] Hence, to solve the Schrödinger equation associated to it,

$$\hat{H}\psi_i(x) = -\frac{1}{2}\nabla^2\psi_i(x) + V_0\left(\left(\frac{x^2}{l^2} - 1\right)^2 - 1\right)\psi_i(x) = \varepsilon_i\psi_i(x) \quad (1)$$

the Hamiltonian was diagonalized in a basis set, $\{c_n\}$, of Hermite orthonormal functions; that is, the solutions of the harmonic oscillator,

$$c_n(x) = \sqrt{\frac{1}{\pi^{(1/2)} n! 2^n}} H_n(x) e^{(-x^2/2)} \quad (2)$$

with $H_n(x)$ Hermite polynomials. The main advantage of using this basis set is that the Hamiltonian matrix is sparse with the only non-zero elements being $H_{n,n}$, $H_{n,n+2}$ and $H_{n,n+4}$.[21] Using the recurrence relations of the Hermite polynomials is simple to show that all integrals that appear in the Hamiltonian matrix are of the type $\int_{-\infty}^{\infty} c_n(x) x^r c_n(x) dx$. These integrals have analytical solutions[22]. In all calculations 100 basis functions were used. The good accuracy of this procedure has been previously shown.[21, 23] The many-electron wavefunction was constructed as a restricted Slater determinant to ensure antisymmetry of the wavefucntion. All linear algebra, numerical integration and plots were prepared with MATHEMATICA.

For our purposes, an analogy between the SDW potential and 1D diatomic molecules[24] (or two sites in a solids) can be established. Each individual well represents a bounding region with a given accessible volume to electrons just as the Coulomb potential does in atoms. The depth of the wells facilitates to tune the relative energy between the last occupied state and the top of the barrier and its shape (height and width). This determines the probability of tunneling and therefore the tendency to delocalize electrons above the barrier. Similarly, the distance between wells and the width of the barrier play a role similar to the distance between atoms in diatomic

molecules and the strength of the confinement/pressure imposed by the environment. This leads to the differentiation of two effects: external potential (type of atom) and pressure.

B. The electronic structure

The structuration of electrons within the SDW potential will be followed with the Electron Localization Function (ELF). ELF is perhaps the descriptor that encodes the Pauli principle most broadly used in quantum chemistry. It derives from $D(\mathbf{r})$,the curvature of conditional density of probability to find two electrons with the same spin at an spherically-averaged distance *s* around a point **r**, $P^{ss}(\mathbf{r},\mathbf{r}+s)$:

$$D(\mathbf{r}) = \frac{1}{2}\nabla_s^2\left(\frac{p^{ss}(\mathbf{r},\mathbf{r}+s)}{r(\mathbf{r})}\right) = \frac{1}{2}\nabla_s^2 P^{ss}(\mathbf{r},\mathbf{r}+s) = \frac{1}{2}\sum_{i=1}^{N}\left|\nabla y_i(\mathbf{r})\right|^2 - \frac{1}{8}\frac{\left|\nabla r(\mathbf{r})\right|^2}{r(\mathbf{r})} \quad (3)$$

where $p^{ss}(\mathbf{r},\mathbf{r}+s)$, $r(\mathbf{r})$ and $y_i^s(\mathbf{r})$ are the same-spin two-particle density matrix, the electron density and the occupied molecular orbitals of a closed-shell Slater determinant. The smallest the probability to find two electrons with the same spin in a region, the more localized the reference electron is.

ELF is defined from the conditional probability, $D(\mathbf{r})$, scaled with respect to the non-interacting homogeneous electron gas value, $D^{HEG}(\mathbf{r})$, and mapped with a Lorentzian function:

$$h(\mathbf{r}) = \left(1+\left(\frac{D(\mathbf{r})}{D^{HEG}(\mathbf{r})}\right)^2\right)^{-1}, \quad (4)$$

so that it runs from 0 to 1. ELF is high in those regions where it is highly likely to find localized pair of electrons. A value close to 0.5 is expected for simple metals because it corresponds to non-interacting homogeneous electron gas.

Eq. (3) can also be interpreted as a kinetic energy density due to the fermionic nature of electrons[25] (aka Pauli kinetic energy density). Indeed, the first term of $D(\mathbf{r})$ in Eq. (3) is the positive definite kinetic energy density of a system with mean-field non-interacting electrons, while the second is the kinetic energy density of a system of bosons with the same density. Therefore, electrons do not localize where $D(\mathbf{r})$ is large because

the Pauli principle locally imposes them high kinetic energy. Within this interpretation, regions of high ELF can be associated with a bosonic behavior, whereas regions of low ELF are due to an "excess" of kinetic energy due to the Pauli exclusion principle.[26]

This second interpretation is the most appropriate for our studies. We are interested in understanding the role the Pauli principle plays on the localization/delocalization of non-interacting confined electrons. However, Eq. (4) needs to be slightly revisited for the 1-dimensional potentials. In this case, the kinetic energy density of the homogeneous electron gas is given by $D_{HEG}^{1D}(x) = \pi^2\rho^3(x)/24$.

Thus, for 1-dimensional systems with compensated spin the ELF reads,

$$h(x) = \left(1 + \left(\frac{\sum_{i=1}^{N/2} \left|\partial_x \gamma_i(x)\right|^2 - \frac{1}{8}\frac{\left|\nabla r(x)\right|^2}{r(x)}}{\frac{\pi^2}{24} r^3(x)} \right)^2 \right)^{-1} \quad (5)$$

In the Hermite basis set used, all terms in Eq. (5) become analytic.

ELF minima in 1D allow defining regions of localization (aka basins, Ω) and their properties, such as the population, $N_W = \int_{x\in W} r(x)dx$.

We will show that coupling the SDW potential with ELF captures the whole range of characteristic electronic structuration upon compression. Moreover, the effects can be dissected beyond the nature of the atoms involved but as a mere interplay of confinement and external potential. This leads to a model for understanding the behavior of bonding under pressure: from atomic solids to metals, and from metals to electrides.

The reason why a local non-periodic potential with non-interacting electrons could be suitable to explain bonding in solids deserves further discussion. Although electron-electron interaction is a big part of the total energy of actual systems, the Pauli principle is a strong organizing principle of the spatial distribution of Fermions. It is so robust that it does not need to appeal to details of Fermion-Fermion interactions to explain the stability of the matter[27] even under extreme conditions such as the inner of super dense starts; neither it needs the electron-electron interactions to reveal the shell structure of

atoms or the general patters of bonding of molecules or solids. A clear example of these is the success of methods such as Hückel and tight binding in molecules and solids.

On the other hand, the near slightness of the matter[28, 29] supports the use of local potentials to reproduce some local and semilocal properties of solids. Kohn and Prodan[28] showed that electron distributions and many response functions "depend on the effective external potential only at nearby points only on the local environment". In a seminal following paper Richard Bader[30] makes the connection between the near slightness of the mater (NEM) and chemistry. NEM sustains concepts of the chemistry such as the transferability of functional groups and local ideas such as atoms and bonds and localizability due to Fermi exchange. A good example of the degree of the locality of electron localization is exponential/algebraic decay of electron localization indexes of insulator/metals with the distance.[31, 32]

III. RESULTS AND DISCUSSION

We have analyzed nine potentials with three different barrier heights (V_0= *8, 16* and *32* E_h) and three different distances between the bottoms of the wells (λ=*1, 2,* and *3* a_o). The most representative examples are collected in the coming sections. All the potentials, state eigenvalues, ELF plots and populations can be found in Figures S1-S4 of Supporting Information (S.I.).

A. Atomic and molecular solids

As a consequence of the Fermi hole, electrons in a system with a bound state tend to form pairs of electrons of opposite spin localized in specific regions of real space (also known as basins within the frame of dynamical system theory usually used for ELF).[33-35] In the case of atoms these regions correspond to electronic shells while for molecules and solids, apart from the electronic shells, the valance space is divided into regions associated with bonds, lone pairs, and lone electrons.[36, 37]

Figures 1a-b show the results of the ELF for 12 electrons trapped in a deep potential, SDW(32,3), i.e. V_0= *32,* λ=*3* (Figure 1a). It should first be noticed that the typical chemical image of atomic shells is recovered within each well (i.e. atom- Figure 1b and 1d). When the last occupied state is well below the barrier (see arrow in Figure 1a), this is inaccessible to electrons. Electrons are perfectly confined in each well. Each

of these sides shows three basins: one between the most external classical returning point and (approximately) the bottom of the well (shaded blue in Figure 1a), a second one between the bottom of the well and a point before the inflection point of the potential (shaded green in Figure 1a), and a third one which is bounded by the top of the barrier (shaded red in Figure 1a).

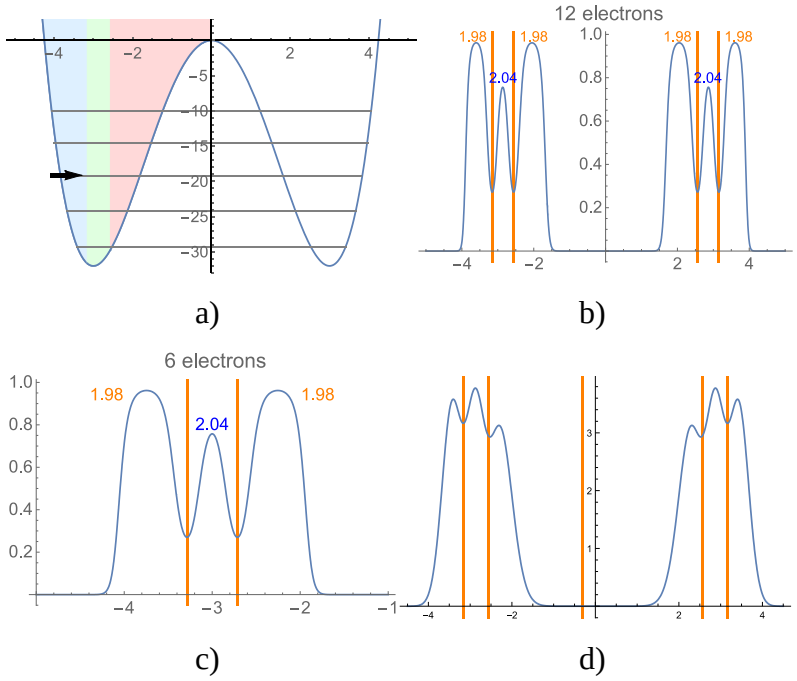

Figure 1. a) SDW potential with V_0= *32* and λ=*3* (SDW(32,3)). The last occupied state for 12 electrons is marked with an arrow. Each shaded region corresponds to an ELF basin. b) ELF for 12 electrons trapped in the SDW(32,3) potential. c) ELF for 6 electrons in the harmonic potential that fits the bottom of the SDW(32,3) potential. d) Electron density for 12 electrons trapped in the SDW(32,3) potential. In b) and c) electron populations of the basins are in orange and blue. Vertical lines in these plots represent the boundaries of the ELF basins.

The number of electrons in each basin is shown in Figure 1b. The 1D symmetric model divides the electrons in shells of ca. 2 electrons each. In 3D, this would correspond to two atoms from the second period, with a central K shell and the L shell around it. Figure 2 shows the results from a real calculation for the LiF solid. Figure 2a shows the 1D ELF around a F^- anion in the solid. A pattern similar to that of Figure 1b arises, with K and L shells. The corresponding 3D picture of the F^- anion in LiF is shown in Figure 2b. Comparison of Figs 1c and 2a shows the agreement at the chemical level between a simple parabolic potential and Coulombic potentials in real systems. Pauli repulsion

dominates the spatial localization so that if there were no Pauli correlation/repulsion, electrons would tend to minimize their potential energy in the SDW by avoiding the barrier. In this case, the number of electrons in the red region (Figure 1a) would be much less than 2. It should be noted that a similar behavior has been observed in electrons in a 1-D box.[38]

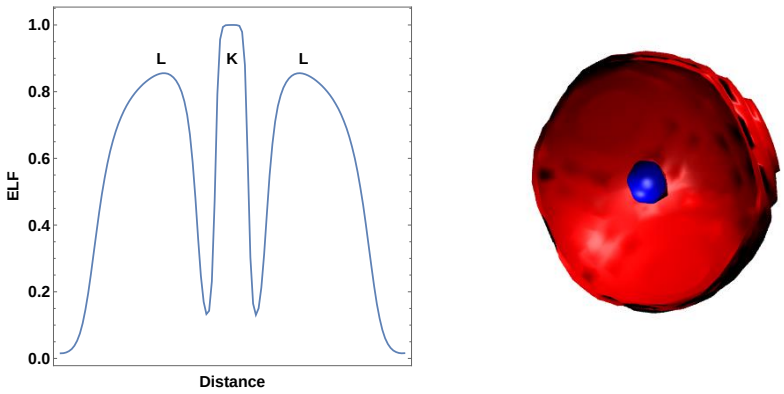

a) b)

Figure 2. a) 1D image for the LiF solid along the bonding line. The 2 shells (K and L) for the F^- anion are shown. Keep in mind that a) comes from a solid state calculation an only the ELF around the F^- anion is shown b) 3D image of the spherical shells in the F^- anion, with K shell in blue and L in red.

When the barrier is high, electrons in each well are only slightly correlated by the Pauli principle. Hence, for strongly confined electrons, each well should behave similarly to a harmonic potential (i.e. free atom). Figure 1c shows the ELF for 6 electrons in the harmonic potential that fits the bottom of the SDW(32,3) potential. They show essentially the same shape (See Figure S5 in S.I.). Only slight differences are observed in the position of the maxima, which in the SDW are displaced towards the barrier. Whereas shells are centered around the minimum of the symmetric parabola in the harmonic approximation, they are displaced towards the barrier in the SDW. This is due to the asymmetric potential within the well, which leads to smaller potentials towards the barrier.

Not only the shape of the ELF of each atom of the 1D molecule (SDW) is preserved in the harmonic approximation, but also the localization length (size of shells in atoms). Within the harmonic approximation of the bottom of the well, a relationship

between the confinement length (L) (green region Figure 1a) and the depth of the well of the potential (atomic number in atoms), V_0, can be established because of the virial theorem of the harmonic potential ($\langle T \rangle = \langle V \rangle$):

$$L \mu \frac{1}{\sqrt{V_0}} \tag{6}$$

Figure 3 shows how this relationship holds for SDW potentials whose states lay well below the barrier. In other words, the shell structuration is at the atomic level, and not affected by neighboring atoms.

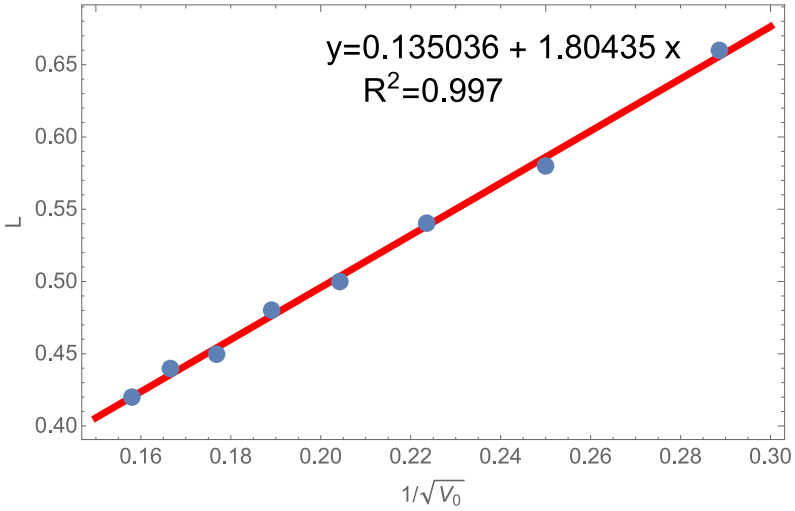

Figure 3. Correlation between the length, L, of confinement (length of the basin associated with the bottom of the well) and the depth of the potential, V_0. This harmonic virial relationship only holds for electrons that are well trapped in the bottom of the potential.

Overall the SDW potential represents a good model of a weakly-interacting atomic or molecular solid, with each atom/molecule preserving its electronic structure and only slightly perturbed by its neighbors. Hence, deep SDW potentials provide a good model for atomic and molecular solids with non-covalent bonds.

B. Delocalization

In the above example, the number of filling electrons has been chosen following the symmetry of the system (two symmetric wells, i.e. 3 basins on each). However, it is

also interesting to analyze the electronic distribution when the number of electrons is not enough to fill these basins with pairs. Figure 4a shows the results for SDW(16,3) with 10 electrons, leading to confined electrons (the last occupied state is marked with an arrow). The following results remain the same if a SDW(32,3) potential is used, but it is more clearly seen in the SDW(16,3). Electrons are more localized at the ends of the potential in the region next to the external classical turning points (shaded blue in Figure 4a-bottom). This is in agreement with the classical limit in which electrons spend more time close to the turning points.[39] One localized pair of electrons (N=1.95) is found in this basin. However, there are ca. 3 electrons left to distribute between the other two basins of the well (green and red in Figure 4a-bottom). This leads to less differentiated maxima and minima of ELF. From the mathematical point of view, this is said to be a less persistent topology.[40] From the physical viewpoint, this means that electrons are more delocalized (i.e. these maxima are less "significant" to identify localization). This is numerically represented by the difference $\Delta ELF = ELF_{max} - ELF_{min}$, so that delocalized regions are identified by a small ΔELF. This localization window is only ΔELF=0.038-0.2 for the maxima involved (shaded green and red), so that these topological regions are not robust and can be rather considered as 3 electrons delocalized over 2 basins. A classic example of a real system with 3 electrons shared between two basins are neighboring π bonds in benzene, where each bond has an average of 1.5 electrons and the localization window between them is 0.2 (see S.I. for further information on this system).[41]

Hence, SDW potentials with an odd number of confined electrons per well lead to delocalized electrons which are the seed for metallization in extended systems.

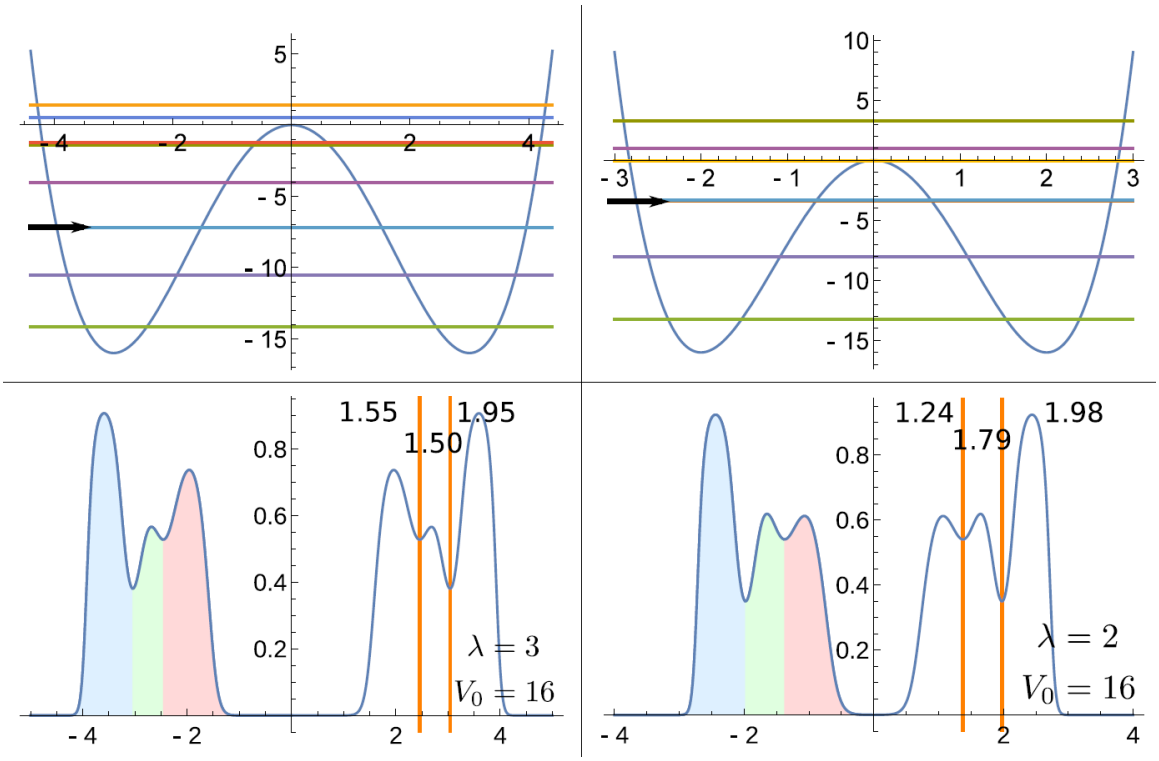

a) b)

Figure 4. Results for SDW(16,3) (a) and SDW(16,2) (b). Top: Symmetric double well potential. The eigenvalues of the non-interacting states are depicted as horizontal lines. The last occupied state for the 10 electrons case is marked with an arrow. Bottom: Electron Localization Function of the symmetric double well potential with 10 electrons. Vertical lines are the boundaries between basins of the ELF. Electron population of the basins is shown over each basin.

C. Metallization

1. Pressure

The distribution of electrons depends on the strength of the confinement. Figure 4b shows the results for a greater confinement for the previous V_0=16 (from λ=3 in Figure 4a to λ=2 in Figure 4b). Confinement progressively leads to a greater delocalization because the rising kinetic energy becomes dominant over the Pauli principle. This is casted with the delocalization window, ΔELF, which further decreases to ΔELF=0.072-0.078 for the maxima involved (shaded green and red in Figure 4b). In other words, we see that confinement in our model promotes the metallic state as in the case of insulating-metal transition induced by pressure (e.g. Mott transition[42] and metallization of Hydrogen) . The possibility to identify such a transformation in real systems was

presented by Silvi and Gatti,[43] who showed that small ΔELF values (flatness of ELF) are a signature of metallic bonding. This was latterly illustrated for iodine metallization under pressure.[44]

2. N-large regime

Taking the same potential as before, SDW(16,2), and increasing the number of electrons allows to model delocalization in an extended system, i.e. a real metal. The ELF and the electron density of the SDW(16,2) potential for 14 to 24 electrons are shown in Figure 5. This potential can hold only 14 electrons below the barrier (Figure 4b. The first three states are doubly pseudo-degenerate). Hence, as the number of electrons grows beyond 14, the system should resemble a homogeneous electron gas (electrons in a box).

Overall, delocalization increases with the number of electrons. This can be seen in the average value of ELF progressively approaching that of the homogeneous electron gas (ELF=0.5). Besides, the number of basins becomes *N/2*, each of them holding 2 electrons.

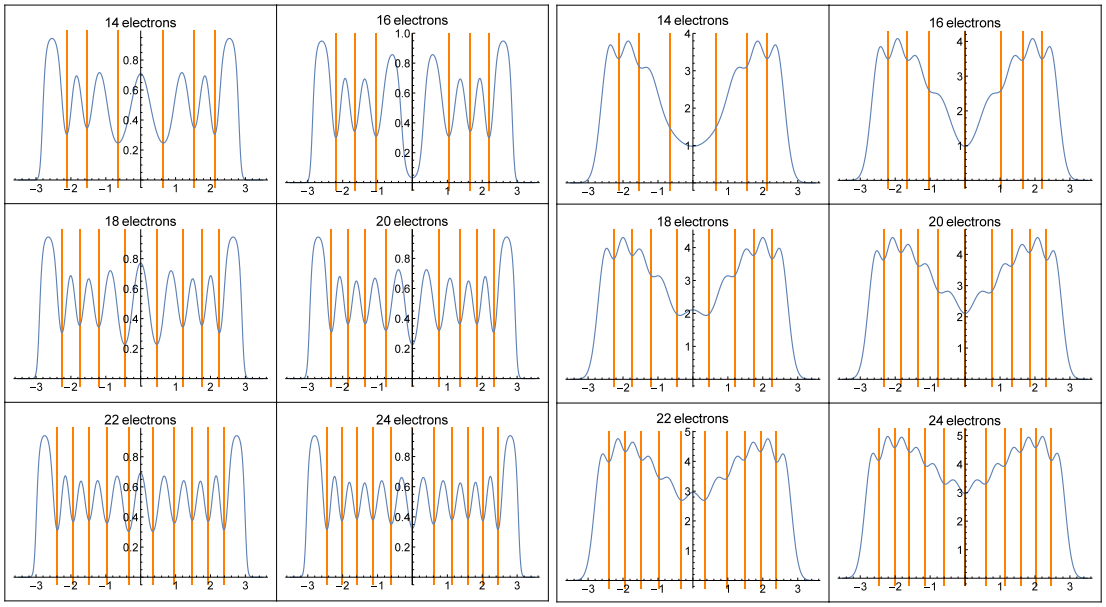

a) ELF b) Electron density

Figure 5. Electron localization function (a) and electron density (b) of a SDW(16,2) potential with 14 to 24 electrons. In all plots vertical lines indicate the points where the density has a minimum.

A correspondence between the minima of the ELF and those of the density emerges in the thermodynamic limit. In the large-*N* limit, a gradient expansion of the kinetic energy density to first order becomes accurate,[45]

$$\sum_{i=1}^{N/2} \left|\nabla_x \psi_i(x)\right|^2 \approx t^{TF}(x) - \frac{1}{3}t^{W}(x) \tag{7}$$

Where the terms are as in Eq 1.2 the 1D Thomas-Fermi kinetic energy density, $t^{TF} = D_{TF}^{1D}$, and the von Weizsacker's one, $t^{W}(x) = \frac{1}{8}\frac{\left|\nabla_x \rho(x)\right|^2}{\rho(x)}$. Replacing Eq. (7) into Eq. (5), it can be shown that the points, $\bar{x}$, where ELF becomes minimal, are given by one of the following conditions (see S.I. for a complete development).

$$\begin{aligned} &\nabla_x \rho = 0 && (a) \\ &\nabla_x \rho = \sqrt{6c}\,\rho^2 && (b) \\ &\nabla_x^2 \rho = 2\frac{(\nabla_x \rho)^2}{\rho} && (c) \end{aligned} \tag{8}$$

Condition (*a*) implies critical points of the density are also critical points of the ELF. Condition (*b*) is satisfied at the $\pm\infty$ where both, the density and its derivative tend to zero. Condition (*c*) constitutes a kind of cusp condition for the electron density at the critical points of the ELF. In other words, in the large-N limit the space partitioning induced by ELF and by the electron density (Atoms In Molecules)[46] become equivalent.

Besides, as the number of electrons above the barrier increases, the ELF profile becomes flatter. In order to better account for the great number of non-persistent maxima, we can resort to an average window to account for this flatness, $F = \langle ELF_{Max} \rangle - \langle ELF_{Min} \rangle$. Figure 6 reveals an increasing of metallization as *F* decreases with the number of electrons.

Overall, we have seen that delocalization is fostered by a mismatch between the number of centers and electron pairs. This is analogous to delocalized bonding patterns in molecules. This effect naturally appears in the solid state where the number of electrons is large and they overcome the barrier. This can be viewed as a good model for bonding in a metallic solid. Since pressure has a direct effect on the barrier, Wigner's principle on pressure-induced metallization appears naturally in our model.

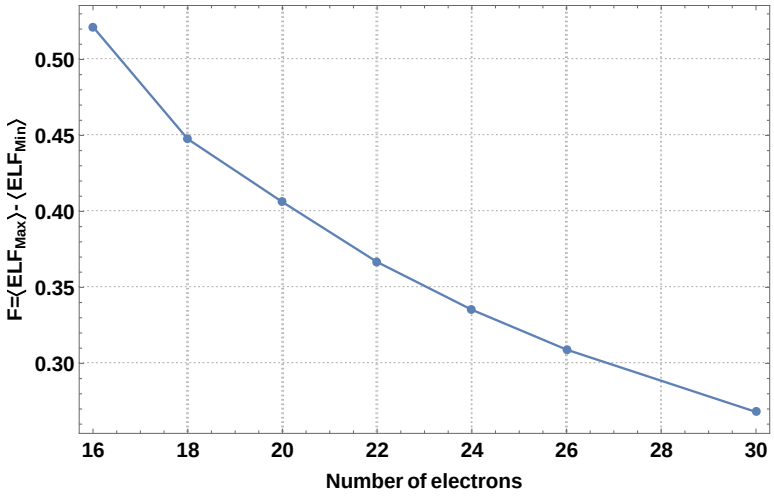

Figure 6. Difference between the mean of the maxima and the mean of the minima of the Electron localization function of a SDW(16,2) potential with 16 to 30 electrons.

4. Electrides

It has been recently shown that metals under very high pressures (5-fold compression) can further undergo electronic reorganization towards what is known as "electrides". Typical s-group metals such as sodium or potassium lead to insulating phases.[47, 48] The ELF picture of these systems has shown that the electron from the last shell becomes localized in a void, leading to "pseudo-ionic" phases.[49] In the case of different external potentials (heteroatoms), the concept is in agreement with the idea of a *pull electride*, where the *s* electron of an alkali atom is pulled away from its valence shell by donor groups.[50]

In order to facilitate the formation of electrides, it is necessary for the electron to be able to escape the atomic attraction, i.e., to go out of the potential well. Hence, we have decreased V_0 to 8 E_h. The resulting potential, SDW(8,2), is depicted in Figure 7a. For this potential, the last occupied state is slightly below the barrier. In this case, there is a large probability of tunneling, and electrons are able to localize on the top of the barrier to reduce the Pauli repulsion with the electron in the basin of the bottom of the well (Figure 7a-medium).

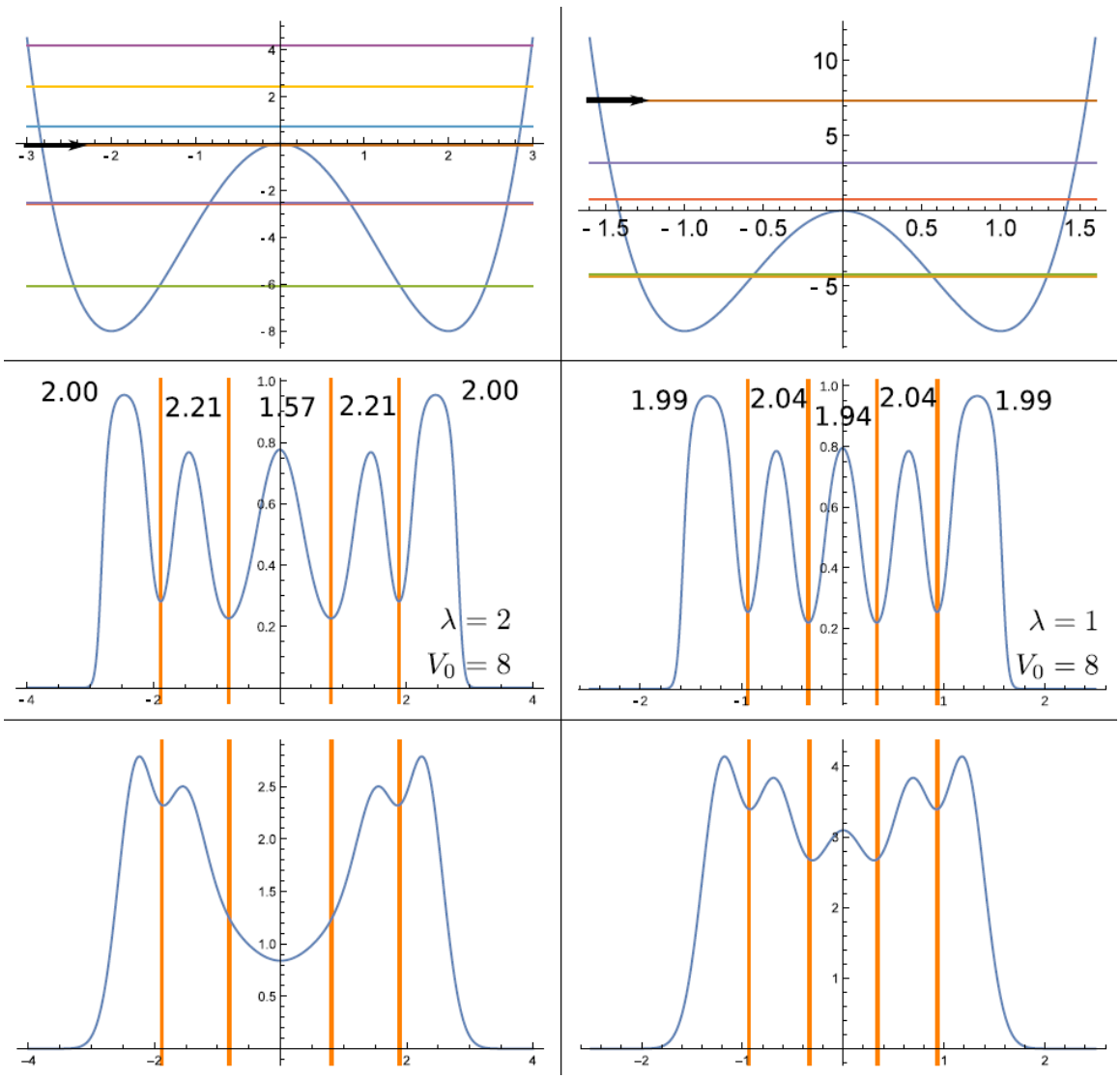

Figure 7. 10 electrons in: a) a SDW(8,2) potential and b) a SDW(8,1) potential. Top: SDW potentials. The eigenvalues of the non-interacting states are depicted as horizontal lines. The last occupied state is marked with an arrow. Medium: Electron Localization Function. Bottom: Electron density. Vertical lines are the boundaries between basins of the ELF. Electron population in orange.

We can further increase the pressure by decreasing the parameter λ to 1 a_0 (SDW(8,1) in Figure 7b). For this potential, the last occupied state is well above the barrier. The ELF is essentially similar to that of SDW(8,2), however, in this case the number of electrons in the basin barrier is very close to an electron pair (1.94 electrons). This shows that not only the localization is high, but that a new electron pair has been

formed at the top of the barrier. An essential difference is observed between both potentials that goes beyond the occupation numbers. Whereas the electron density is minimal at the top of the barrier for SDW(8,2) (Figure 7a-Bottom), it is maximal on the top of the barrier for the SDW(8,1) potential (Figure 7b-Bottom). This is a basic characteristic of electrides: electrons form a pseudo-anion, which is identified by both the electron density and ELF attaining a maximum.[50] Hence, low barriers and small inter-well distances are a good model for electride behavior. Results for a real system (potassium) are shown in Figure 8. At low pressure, a flat ELF profile is obtained like the one modelled with SDW(16,2) (Figures 4 and 5). The increase of pressure results in the valence electrons flowing towards the interstices, while atoms conserve their shell structuration. This new state of matter is the one we have modeled with SDW(8,1) potential in Figure 7b.

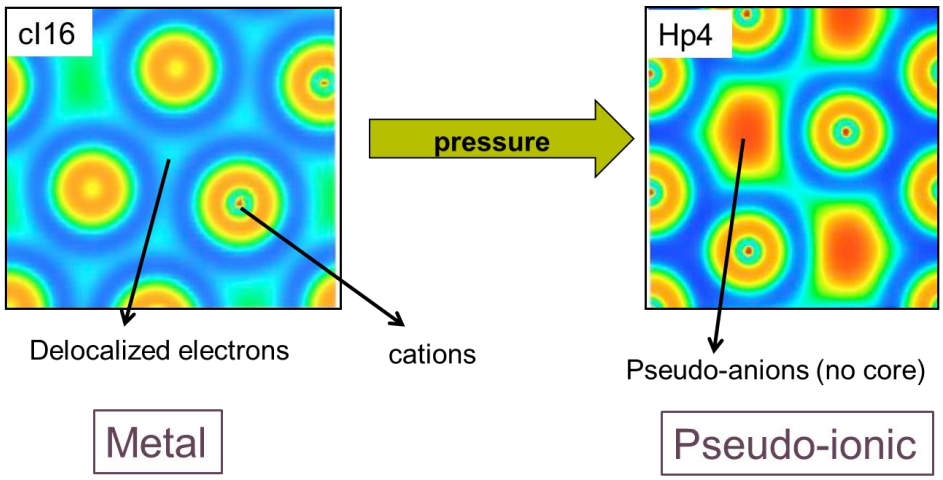

Figure 8. Evolution of ELF of potassium under pressure. Electrons are initially delocalized (flat ELF profile) in the metallic phase and become localized in the voids in the pseudo-ionic phase.

Alternatively, one can make an analogy between the basin in the most attractive part of the well and those regions in solids and molecules where the nuclear potential is more attractive (Berlin's bonding regions: core, lone pairs and bonds)[51]. This means that electrons in electrides occupy a classically forbidden region (non-bonding Berlin's regions). Then, it may be useful to think in the localization of the electron in an electride as a balance between Pauli electron-electron repulsion and electron tunneling. We are

currently further exploring this idea in real molecular electrides by computing approximations to quantum potential of electrons.

IV CONCLUSIONS

Summarizing, this simple example of non-interacting electrons in the one dimensional SDW potential shows the importance of the Pauli exclusion principle, the external potential and confinement to explain the localization/delocalization of electrons under pressure. At normal pressure it recovers the organization into atomic shells around each well. With increasing pressure, the increasing kinetic energy destroys the effective pairing of electrons yielding a high fluctuation of the population of the basins of the ELF. Moreover, in the limit of large number of electrons, the pattern of localization approaches the one of the homogeneous gas and it is shown that there is a correspondence between ELF and density topologies. As the kinetic energy keeps increasing, ELF also captures the probability of tunneling of electrons populating states below the top of the barrier. When the kinetic energy is high enough, pairing is once again favorable and density concentrates in the classical forbidden region. This is in analogy to the transition from metals to electrides.

Supporting Information

The following data are collected in Supported Information, accessible free of charge:
Potentials and state eigenvalues for all combinations of V_0= 8, 16 and 32 E_h and λ=1, 2, and 3 a_o. ELF profiles for all combinations of V_0= 8, 16 and 32 E_h and λ=1, 2, and 3 a_o. Populations for all combinations of V_0= 8, 16 and 32 E_h and λ=1, 2, and 3 a_o. Electron density profile of V_0= 8, 16 and 32 E_h and λ=1, 2, and 3 a_o. Comparison of the SDW(32,3) and the harmonic approximation for a single well. Method details. Benzene π electrons: the 3 electrons-2 centers case. Demonstration of ELF and electron density topologies coalescence

Acknowledgments.

This work was financed by: i) FONDECYT through projects No 1181121 and 1180623, ii) ECOS C17E09, and iii) Centers Of Excellence With Basal/Conicyt Financing, Grant FB0807

REFERENCES.

[1] A. Sarsa, and C. Le Sech, J Chem Theory Comput **7**, 2786 (2011).
[2] J. Cioslowski, and E. Matito, J Chem Theory Comput **7**, 915 (2011).
[3] P. F. McMillan, Chemical Society Reviews **35**, 855 (2006).
[4] W. Grochala, R. Hoffmann, J. Feng, and N. W. Ashcroft, Angewandte Chemie International Edition **46**, 3620 (2007).
[5] K. Amaya, K. Shimizu, and M. Eremets, International Journal of Modern Physics B **13**, 3623 (1999).
[6] H. P. Scott, Q. Williams, and E. Knittle, Physical Review Letters **88**, 015506 (2001).
[7] E. Wigner, and H. á. Huntington, The Journal of Chemical Physics **3**, 764 (1935).
[8] J. L. Dye, Accounts of chemical research **42**, 1564 (2009).
[9] B. G. Janesko, G. Scalmani, and M. J. Frisch, J Chem Theory Comput **12**, 79 (2016).
[10] M. Marqués, G. J. Ackland, L. F. Lundegaard, G. Stinton, R. J. Nelmes, M. I. McMahon, and J. Contreras-García, Physical Review Letters **103**, 115501 (2009).
[11] R. J. Hemley, High Pressure Research **30**, 581 (2010).
[12] M. Munoz, and C. Cardenas, Phys Chem Chem Phys **19**, 16003 (2017).
[13] C. Cardenas, W. Tiznado, P. W. Ayers, and P. Fuentealba, The Journal of Physical Chemistry A **115**, 2325 (2011).
[14] C. Cardenas, Chem Phys Lett **513**, 127 (2011).
[15] O. A. von Lilienfeld, J. Chem. Phys.. **131**, 164102 (2009).
[16] O. A. von Lilienfeld, and M. E. Tuckerman, J Chem Phys **125**, 154104 (2006).
[17] P.-O. Löwdin, Reviews of Modern Physics **35**, 724 (1963).
[18] R. P. Bell, *The tunnel effect in chemistry* (Springer, 2013).
[19] R. d. L. Kronig, Proc. R. Soc. London, Ser. A **130**, 499 (1931).
[20] V. Jelic, and F. Marsiglio, European Journal of Physics **33**, 1651 (2012).
[21] L. A. Verguilla-Berdecia, J. Chem. Educ **70**, 928 (1993).
[22] G. Szegö, New York (1939).
[23] N. Mukherjee, A. Roy, and A. K. Roy, Annalen der Physik **527**, 825 (2015).
[24] P.-F. Loos, C. J. Ball, and P. M. Gill, Phys Chem Chem Phys **17**, 3196 (2015).
[25] A. Savin, B. Silvi, and F. Colonna, Can J Chem **74**, 1088 (1996).
[26] A. Savin, A. D. Becke, J. Flad, R. Nesper, H. Preuss, and H. G. Vonschnering, Angewandte Chemie **30**, 409 (1991).
[27] E. H. Lieb, Rev.Mod.Phys. **48**, 553 (1976).
[28] E. Prodan, and W. Kohn, Proceedings of the National Academy of Sciences of the United States of America **102**, 11635 (2005).
[29] E. Prodan, Physical Review B **73**, 085108 (2006).

[30] R. F. Bader, The Journal of Physical Chemistry A **112**, 13717 (2008).
[31] A. Gallo-Bueno, E. Francisco, and A. M. Pendás, Phys Chem Chem Phys **18**, 11772 (2016).
[32] A. Gallo-Bueno, M. Kohout, and A. Martín Pendás, J Chem Theory Comput **12**, 3053 (2016).
[33] R. J. Gillespie, and R. S. Nyholm, Quarterly Reviews, Chemical Society **11**, 339 (1957).
[34] W. L. Luken, and J. C. Culberson, International Journal of Quantum Chemistry **22**, 265 (1982).
[35] R. F. Bader, S. Johnson, T.-H. Tang, and P. Popelier, The Journal of Physical Chemistry **100**, 15398 (1996).
[36] A. Savin, R. Nesper, S. Wengert, and T. F. Fassler, Angewandte Chemie **36**, 1809 (1997).
[37] M. Kohout, International Journal of Quantum Chemistry **97**, 651 (2004).
[38] P. Fuentealba, D. Guerra, and A. Savin, in *Chemical Reactivity Theory* (CRC Press, 2009).
[39] L. D. Landau, and E. Lifschic, *Course of theoretical physics. vol. 1: Mechanics* (Oxford, 1978).
[40] H. Edelsbrunner, and J. Harer, *Computational topology: an introduction* (American Mathematical Soc., 2010).
[41] T. B. Tai, V. T. T. Huong, and M. T. Nguyen, in *Structure, Bonding and Reactivity of Heterocyclic Compounds* (Springer, 2014), pp. 161.
[42] N. Mott, Reviews of Modern Physics **40**, 677 (1968).
[43] B. Silvi, and C. Gatti, The Journal of Physical Chemistry A **104**, 947 (2000).
[44] A. Savin, Journal of Physics and Chemistry of Solids **65**, 2025 (2004).
[45] A. Holas, and N. H. March, Philosophical Magazine B-Physics of Condensed Matter Statistical Mechanics Electronic Optical and Magnetic Properties **69**, 787 (1994).
[46] R. F. W. Bader, *Atoms in Molecules: A Quantum Theory* (Clarendon, Oxford, 1990).
[47] Y. Ma, M. Eremets, A. R. Oganov, Y. Xie, I. Trojan, S. Medvedev, A. O. Lyakhov, M. Valle, and V. Prakapenka, Nature **458**, 182 (2009).
[48] M. Marqués, M. Santoro, C. L. Guillaume, F. A. Gorelli, J. Contreras-García, R. T. Howie, A. F. Goncharov, and E. Gregoryanz, Physical Review B **83**, 184106 (2011).
[49] M. Marqués, G. Ackland, L. Lundegaard, G. Stinton, R. Nelmes, M. McMahon, and J. Contreras-García, Physical review letters **103**, 115501 (2009).
[50] V. Postils, M. Garcia-Borràs, M. Solà, J. M. Luis, and E. Matito, Chemical Communications **51**, 4865 (2015).
[51] D. Chakraborty, C. Cárdenas, E. Echegaray, A. Toro-Labbe, and P. W. Ayers, Chem Phys Lett **539–540**, 168 (2012).